ISSN 2669-2023 (print) / ISSN 2538-8959 (on-line) / **https://doi.org/10.47459/cndcgs.2026.20**

Experimental Verification of Standardized Explosive Charges for Research into the Effects of Blast Waves on People and Structures During Explosive Tactical Breaching

Jakub VRBKA[1]*, Jiří ŠTOLLER[1], Klára CIBULOVÁ[1], Pavel MAŇAS[1], Petr DVOŘÁK[1], Michal BILINA[2]

[1]Department of Engineering Technology, Faculty of Military Technology, University of Defence, Kounicova 65, Brno 66210, Czech Republic
[2]Department of Engineer Support, Faculty of Military Leadership, University of Defence, Kounicova 65, 66210, Brno, Czech Republic

*Correspondence:*jakub.vrbka@unob.cz*

Abstract

This paper addresses the problem of experimental reproducibility in the study of blast effects during explosive tactical breaching. In real conditions, breaching charges exhibit significant variability, which complicates the comparison of measured pressure responses and limits systematic research. The study investigates whether real breaching charges can be replaced by standardized spherical charges with an equivalent TNT effect. Experimental measurements were carried out in a training facility using pressure sensors, and the results were evaluated in terms of peak overpressure, impulse, and pressure-time history. The findings indicate that standardized charges provide comparable blast characteristics, with differences within acceptable limits. The proposed approach enables more reproducible experiments and creates a basis for further research on structural resilience and human exposure to repeated blast loading.

KEY WORDS: *explosive breaching, blast wave, overpressure, impulse, structural resilience, experimental standardization, additive manufacturing*

Citation: Vrbka, J.; Štoller, J.; Cibulová, K.; Maňas, P.; Dvořák, P.; Bilina, M. (2026). Experimental Verification of Standardized Explosive Charges for Research into the Effects of Blast Waves on People and Structures During Explosive Tactical Breaching. In Proceedings of the Challenges to National Defence in Contemporary Geopolitical Situation, Brno, Czech Republic, 7-10 September 2026. ISSN 2538-8959, https://doi.org/10.47459/cndcgs.2026.20

1. Introduction

The effects of blast waves represent a key area not only in military operations but also in the design and assessment of structures subjected to extreme loading conditions. The propagation of blast waves in air and their interaction with structures have been extensively described in the literature [1–5]. These effects are associated not only with structural damage but also with potential injury mechanisms affecting exposed individuals [6–11]. In confined or semi-confined environments, such as building interiors, the blast wave is significantly modified due to reflections and interactions with structural boundaries. This results in complex pressure fields characterized by multiple peaks and prolonged duration, as demonstrated in previous experimental and numerical studies [15–19].

One typical scenario where these aspects overlap is Explosive Tactical Breaching. During this activity, the members of the team, the people inside the building, and the building structure itself are simultaneously exposed to the effects of the explosion. However, for the purposes of experimental research, the use of real breaching charges is problematic in terms of variability, availability, and economics. The basic requirement for scientific research is reproducibility, which is difficult to achieve with relatively variable breaching charges. This paper therefore addresses the question of whether original breaching charges can be replaced by standardized spherical charges of plastic explosive with an equivalent TNT effect without distorting the measured results.

2. Methods

Peer-review under responsibility of General Jonas Žemaitis Miltitary Academy of Lithuania and University of Defence, Czech Republic.

2.1. Experimental Setup

Experimental measurements were performed in a training facility within a reinforced concrete building under indoor conditions. Blast pressure measurements were performed using high-frequency pressure sensors, following approaches commonly used in experimental blast research [12]. The sensors were positioned in the interior space at a height corresponding to the charge location (Fig. 1), ensuring consistent measurement conditions within each experiment.

The sensors were mounted on tripods (Fig. 2) to ensure a stable position and repeatable measurement conditions. The measurement chain consisted of high-frequency pressure transducers with a suitable measurement range and sensitivity to capture the dynamic overpressure generated during the explosion.

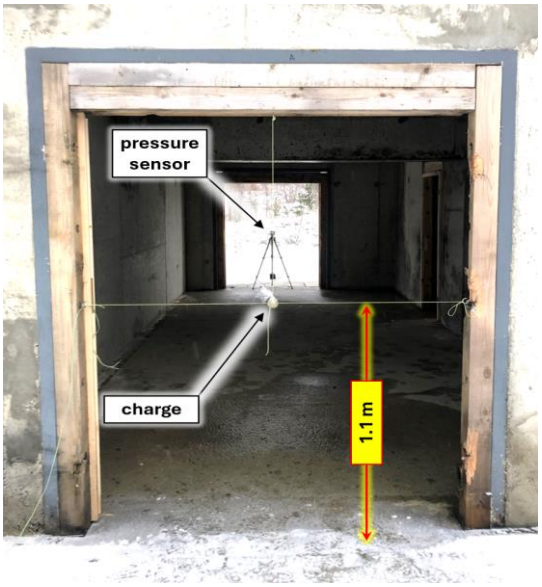

Fig. 1 Experimental setup inside the test facility showing the relative position of the pressure sensor and explosive charge

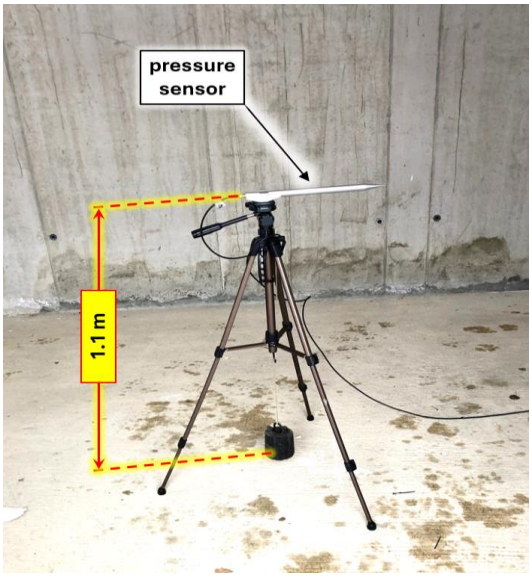

Fig. 2 Pressure sensor mounted on tripod at 1.1 m above the floor

2.2. Explosions and Environmental Conditions

As shown in Table 1, each experimental series consisted of three subsequent explosions: a standardized spherical charge, a real breaching charge, and a repeated standardized charge. This arrangement allows for the simultaneous assessment of both the consistency among the different types of charges and the repeatability of the standardized charges. Within each experimental series, the position of all sensors was maintained for all three explosions. However, the sensor layout was changed between individual experiments. Direct comparisons between charge types were therefore always performed only within the same series, i.e., under identical measurement configuration.

Table 1

Summary of test configurations and measured environmental parameters

Experiment	Explosion	Type of charge	TNT mass [g]	Temperature [°C]	Atmospheric pressure [hPa]	Relative humidity [%]
①	1.1.	Standardized spherical	100	0.2	922.8	93.0
	1.2.	Real breaching		-0.4	923.1	98.0
	1.3.	Standardized spherical		-0.5	923.2	99.2
②	2.1.	Standardized spherical	100	-0.6	923.5	99.1
	2.2.	Real breaching		-0.8	923.6	99.9
	2.3.	Standardized spherical		-0.4	923.8	99.9
③	3.1.	Standardized spherical	20	-0.6	924.1	99.9
	3.2.	Real breaching		-0.3	924.2	99.9
	3.3.	Standardized spherical		-0.3	924.1	99.9

The environmental conditions during each explosion were monitored using a TESTO 480 device. Air temperature, atmospheric pressure, and relative humidity were recorded. The measured values are summarized in Table 1. The temperature ranged from −0.8 to 0.2 °C, while atmospheric pressure ranged from 922.8 to 924.2 hPa. These differences are considered negligible and are not expected to have a significant effect on the measured shock wave parameters.

2.3. Charges and Manufacturing

Two types of charges were used in the experiments: actual breaching charges and standardized spherical charges designed as their experimental equivalents. An illustration of the charges is shown in Figure 3.

Standardized charges were created using a plastic explosive (SEMTEX 90PH) in the shape of a sphere with a determined TNT equivalent. To ensure geometric consistency and repeatability, these charges were manufactured using 3D-printed molds, parts of which are shown in Figure 4. This approach allowed for precise control of the charge's geometry and mass distribution.

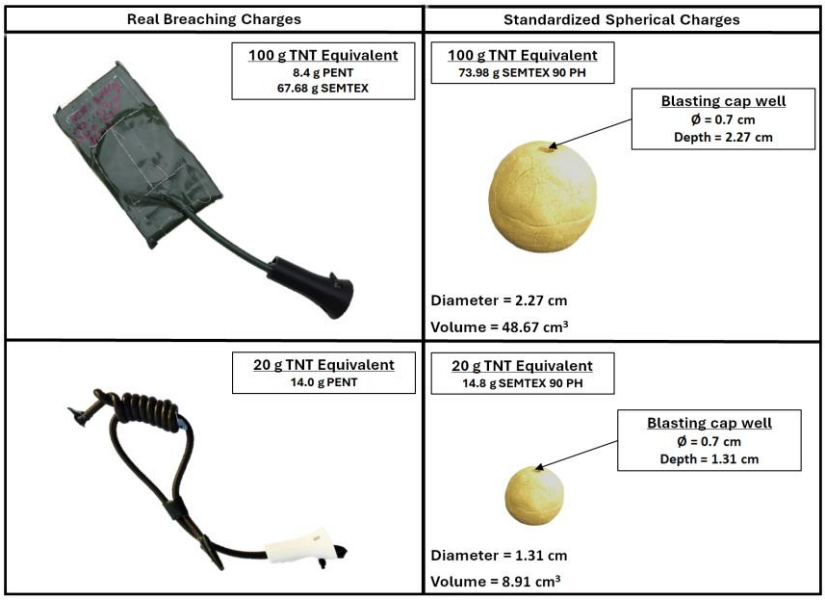

Fig. 3 Comparison of real breaching charges and standardized spherical charges used in the experiments, including both 100 g and 20 g TNT equivalent configurations. The figure illustrates differences in geometry, composition, and manufacturing approach, as well as the defined dimensions and blasting cap placement used for the standardized spherical charges.

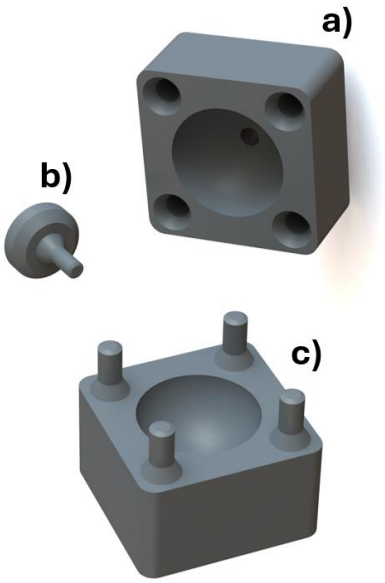

Fig. 4 Design of the mold for standardized spherical charges: (a) main mold body with spherical cavity, (b) insert for blasting cap positioning, (c) assembled mold with alignment pins.

Real breaching charges were used as a reference case for comparison. The experimental design allows for a direct assessment of the equivalence between real and standardized charges under identical conditions.

2.4. Comparison Metrics

A comparison of real breaching charges and standardized spherical charges was conducted based on three sets of metrics, which together allow for a comprehensive assessment of the equivalence of the loads:

2.4.1. Primary Metrics

The primary evaluation parameters are the maximum overpressure p_{max} and the positive impulse I_+, which characterize the intensity and energy effect of the impact load on the structure. The relative differences between the standardized and actual loads were expressed as a relative difference (Δ):

$$\Delta = \frac{x_{eq} - x_{orig}}{x_{orig}} \cdot 100\% \quad (1)$$

where: x_{eq} – the value corresponding to the standardized charge; x_{orig} – the value measured for the real breaching charge.

These metrics were selected because they are directly related to the mechanical effect of the load on the structure and its response.

2.4.2. Dynamic Metrics

To further assess the dynamics of the pressure response, the shock wave arrival time $t_{arrival}$ and the time to reach maximum overpressure t_{peakt} were evaluated.

These metrics provide information on the propagation speed of the shock wave and the load dynamics. While $t_{arrival}$ is primarily related to the wave's propagation through space, t_{peak} reflects the effects of the shock wave's interactions with the environment, particularly in confined spaces.

2.4.3. Shape Metrics

To evaluate the similarity of time series, the Root Mean Square Error (RMSE) and Pearson's correlation coefficient *R* were used. *RMSE* was defined as:

$$RMSE = \sqrt{\frac{1}{N}\sum_{i=1}^{N}(x_{eq,i} - x_{orig,i})^2} \tag{2}$$

where: $x_{eq,i}$ and $x_{orig,i}$ – values of the compared variable in the standardized and reference time series; N – number of samples.

To ensure comparability between individual measurements, the *RMSE* was normalized relative to the maximum value of the reference signal:

$$NRMSE = \frac{RMSE}{x_{\max,orig}} \tag{3}$$

Pearson's correlation coefficient *R* was calculated as follows:

$$R = \frac{\sum_{i=1}^{N}(x_{eq,i} - \tilde{x}_{eq}) \cdot (x_{orig,i} - \tilde{x}_{orig})}{\sqrt{\sum_{i=1}^{N}(x_{eq,i} - \tilde{x}_{eq})^2 \cdot \sum_{i=1}^{N}(x_{orig,i} - \tilde{x}_{orig})^2}} \tag{4}$$

where: $\tilde{x}_{eq}$ and $\tilde{x}_{orig}$ represent the average values of the corresponding signals.

Shape metrics serve as supplementary indicators and allow for an assessment of the similarity of response curves beyond the scope of basic physical parameters. However, their interpretation is always relative to the main metrics p_{max} and I_+, which represent the primary criteria for load equivalence.

3. Results

3.1.1. Primary Physical Parameters of the Load

The maximum overpressure p_{max} and positive impulse I_+ were determined for all tests and measurement points. The values obtained for standardized charges are compared with the results of actual blasting charges in all cases studied. An overview of the results is provided in Table 2.

Table 2

Comparison of peak overpressure and positive impulse between original and equivalent charges

Experiment	Sensor	p_{max} [kPa]			I_+ [kPa·ms]		
		Breaching ch.	Standardized ch.	Δp_{max} [%]	Breaching ch.	Standardized ch.	ΔI_+ [%]
①	P1	10.632	9.362	-11.949	246.188	209.568	-14.875
	P2	4.713	3.209	-31.899	101.697	85.159	-16.262
	P3	10.465	10.512	0.457	140.993	137.670	-2.357
	P4	11.712	9.860	-15.816	210.352	184.482	-12.298
②	P1	10.673	8.627	-19.168	209.407	182.197	-12.994
	P2	5.616	5.590	-0.469	121.523	106.712	-12.188
	P3	8.819	12.348	40.011	158.518	135.115	-14.763
	P4	13.102	10.486	-19.969	217.156	200.779	-7.541
③	P1	4.294	5.506	28.245	74.268	67.074	-9.686

	P2	5.548	5.053	-8.915	95.318	90.054	-5.522
	P3	9.873	9.262	-6.189	104.033	95.764	-7.949
	P4	10.285	14.862	44.497	116.625	95.897	-17.773

3.1.2. Duration Parameters

The shock wave arrival times $t_{arrival}$ are nearly identical in all cases. The time at which the maximum overpressure is reached t_{peakt} shows slight variability depending on the measurement location.

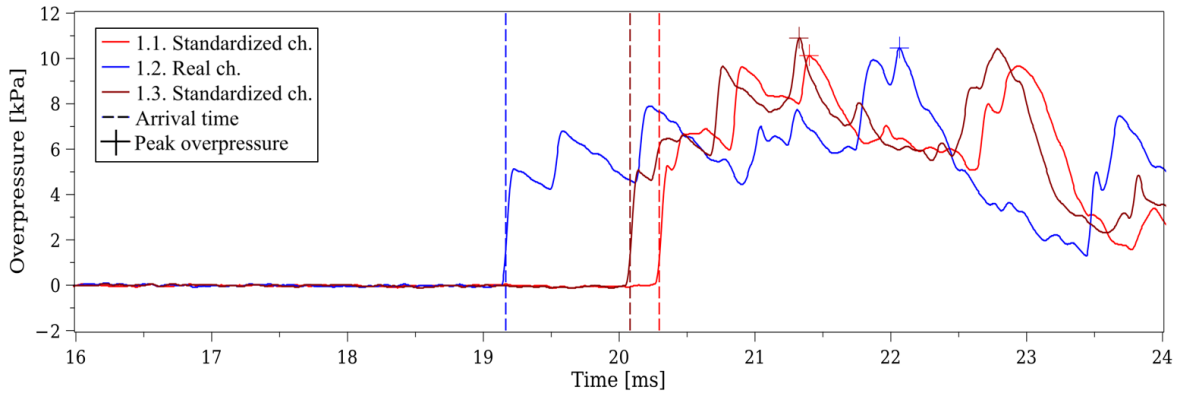

Fig. 5 Pressure curve segment (16–24 ms) from Experiment ① recorded by sensor P3

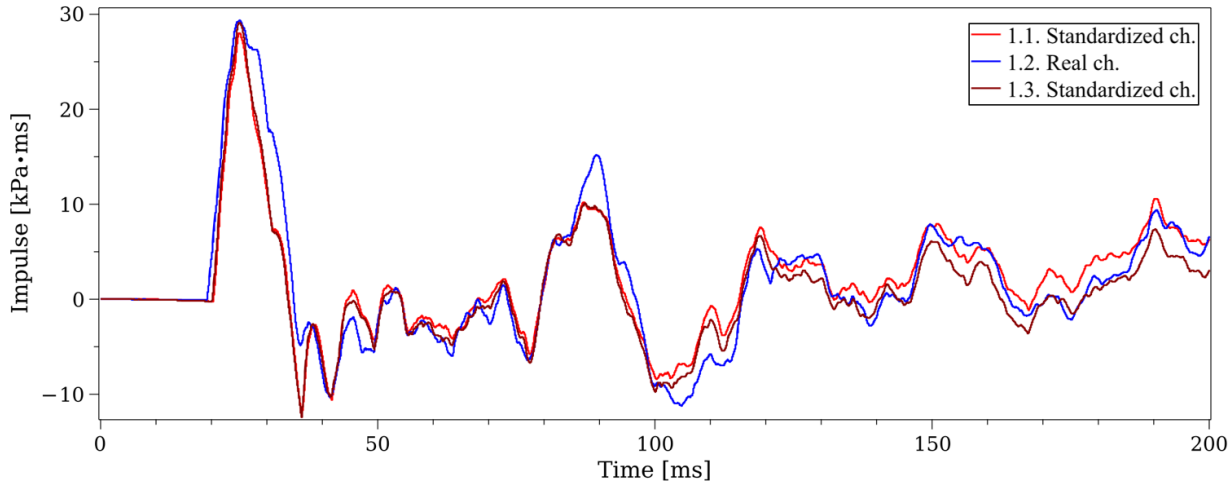

Fig. 6 The pulse waveform from Experiment ① on sensor P3 throughout the entire duration of the signal (200 ms)

The results are summarized in Table 3.

Table 3

Comparison of arrival time and peak time of pressure signals

Experiment	Sensor	$t_{arrival}$ [ms]			t_{peak} [ms]		
		Breaching ch.	Standardized ch.	$\Delta t_{arrival}$ [%]	Breaching ch.	Standardized ch.	Δt_{peak} [%]
①	P1	23.760	23.785	0.025	105.250	105.365	0.115
	P2	14.800	15.730	0.930	97.305	35.155	-62.150
	P3	19.165	20.090	0.925	22.065	21.380	-0.685
	P4	13.350	13.575	0.225	26.360	15.410	-10.950
②	P1	36.690	37.535	0.845	45.200	45.960	0.760
	P2	16.665	17.215	0.550	78.405	60.800	-17.605
	P3	19.205	20.240	1.035	21.585	22.775	1.190
	P4	11.305	12.125	0.820	46.505	27.790	-18.715
③	P1	15.805	15.830	0.025	15.875	22.170	6.295

	P2	19.855	20.085	0.230	37.685	38.230	0.545
	P3	10.985	11.180	0.195	23.275	18.590	-4.685
	P4	7.325	7.440	0.115	16.310	16.340	0.030

3.1.3. Similarity of Trends

The similarity of the pressure waveforms was evaluated using the *RMSE* metric and Pearson's correlation coefficient *R*. A summary of the results is presented in Table 4.

Table 4

Similarity metrics of pressure-time and impulse-time histories

Experiment	Sensor	pressure p			impulse I		
		RMSE [kPa]	*NRMSE* [–]	*R* [–]	*RMSE* [kPa·ms]	*NRMSE* [–]	*R* [–]
①	P1	1.449	0.1363	0.8904	9.337	0.0379	0.9665
	P2	0.870	0.1846	0.7251	2.916	0.0287	0.9749
	P3	1.394	0.1332	0.7558	2.330	0.0165	0.9580
	P4	2.029	0.1732	0.7164	5.775	0.0275	0.9228
②	P1	1.771	0.1659	0.7969	7.308	0.0349	0.9819
	P2	1.214	0.2162	0.6492	3.018	0.0248	0.9851
	P3	1.709	0.1938	0.6599	3.405	0.0215	0.9381
	P4	2.062	0.1573	0.7027	4.415	0.0203	0.9522
③	P1	0.597	0.1391	0.8101	1.472	0.0198	0.6472
	P2	0.898	0.1618	0.7341	2.181	0.0229	0.7830
	P3	0.903	0.0915	0.7810	2.240	0.0215	0.8348
	P4	0.980	0.0952	0.7777	11.436	0.0981	0.0974

4. Discussion

The results of experimental measurements show that the feasibility of replacing real breaching charges with standardized spherical charges depends on the evaluation parameter chosen. While some parameters show good agreement, others are significantly influenced by local conditions and exhibit greater variability.

The most significant differences were observed in the maximum overpressure p_{max}, where relative deviations vary widely and, in some cases, exceed 30–40%. This result confirms that the maximum overpressure is highly sensitive to the details of the charge geometry, its orientation, and, above all, to the complex interaction of the shock wave with the interior structure. In an enclosed space, multiple reflections and interferences occur, which can lead to local amplification or, conversely, attenuation of pressure peaks. For this reason, maximum overpressure does not appear to be a robust parameter for assessing the equivalence of charges. Similar behavior has been reported in previous studies dealing with blast wave propagation in enclosed or partially confined spaces [15–18].

In contrast, the positive impulse I_+ exhibits significantly more stable behavior. The relative deviations between actual and standardized loads range from approximately 5% to 15% in most cases. This confirms that impulse represents a more robust parameter for evaluating blast loading, as it integrates both the magnitude and duration of the pressure signal, which is consistent with established blast theory [1, 2, 20].

Analysis of the time parameters further shows that the time of arrival of the pressure wave $t_{arrival}$ is highly reproducible across different types of charges. In contrast, the time of maximum overpressure t_{peak} exhibits significant deviations in some cases, which is again related to the complex evolution of the pressure response in a confined space and the influence of reflected waves.

The evaluation of the similarity of entire time histories represents a significant contribution. While pressure histories show only a moderate degree of agreement (with correlation coefficients of approximately 0.65–0.90), impulse histories achieve significantly better results. The normalized impulse error is low (on the order of a few percent), and the correlation exceeds 0.9 in most cases. This confirms that the cumulative development of the load over time is reproduced much more reliably than the instantaneous pressure characteristics.

At the same time, however, cases have been identified—particularly with lower payloads and specific sensor positions—where the correlation of the impulse responses is reduced. A summary of the evaluated similarity metrics across all experiments is presented in Table 5. These deviations can be interpreted as a consequence of local phenomena such as reflections, interference, and spatial inhomogeneity of the pressure field. This finding emphasizes that even though the global effect of the load is captured well, the local dynamics may remain partially different.

From an application perspective, these results are significant for both structures and individuals exposed to the effects of an explosion. The response of structures is primarily influenced by the magnitude of the impulse, which

determines the transferred energy and the resulting deformation or damage. From the perspective of human exposure, the temporal characteristics of the blast wave—particularly impulse and duration—are considered key factors influencing injury risk. Previous studies have shown that these parameters are closely related to mechanisms of primary blast injury, including traumatic brain injury [8–11]. Good agreement in impulse values therefore suggests that standardized charges may be a suitable tool not only for studying structural response but also for assessing human exposure under controlled conditions.

Table 5

Summary of similarity metrics between real breaching charges and standardized spherical charges, expressed as mean values across all experiments and sensors.

Metric	Mean deviation	Standard deviation	Interpretation
Relative difference in maximum overpressure Δp_{max} [%]	~20.00	high	low agreement
Relative difference in positive phase impulse ΔI_+ [%]	~10.00	low	good agreement
Difference in arrival time $\Delta t_{arrival}$ [%]	~0.50	low	very good agreement
Difference in peak overpressure time Δt_{peak} [%]	~9.00	high	low agreement
Normalized RMSE of overpressure $NRMSE_p$ [–]	~0.15	moderate	moderate agreement
Pearson correlation coefficient of overpressure R_p [–]	~0.75	moderate	moderate agreement
Normalized RMSE of impulse $NRMSE_I$ [–]	~0.03	low	very good agreement
Pearson correlation coefficient of impulse R_I [–]	~0.90	high	very good agreement

However, it is important to emphasize the limitations of using standardized spherical charges when studying the specific effects of explosive breaching. These charges do not replicate the fragmentation, directionality of the effect, or interaction with structural elements that are typical of real breaching charges. Fragments and detonation products can significantly affect local structural loads as well as the risk of injury to personnel.

Overall, it can be concluded that standardized spherical charges represent a suitable and reproducible alternative for experimental research into the effects of explosions, particularly when evaluating global load characteristics. However, their use must be accompanied by an awareness of the limitations in interpreting local pressure phenomena.

Conclusions

The results show that standardized spherical charges can reproduce the overall effect of an explosion with good accuracy, particularly in terms of positive impulse. While the maximum overpressure exhibits significant variability, the impulse is reproduced more consistently and with smaller deviations. Similarity metrics confirm that impulse time histories exhibit greater agreement than pressure time histories, which underscores the importance of impulse as a key load parameter. These findings are relevant not only for evaluating structural responses but also for assessing the effects of explosions on people, where the impulse and the time history of the load significantly influence the degree of exposure and the risk of injury. Standardized charges thus represent a suitable tool for the reproducible experimental evaluation of explosion effects in the broader context of safety and resilience.

Acknowledgements. This work was conducted within the framework of the Specific Research of the Ministry of Education, Youth and Sport of the Czech Republic: "Explosion Dynamics and Structural Degradation: Prediction of Building Service Life in Breaching Training Area".

References

1. **Kinney G.F., Graham K.J.** Explosive Shocks in Air. Springer, New York, 1985.
2. **Baker W.E., Cox P.A., Westine P.S., Kulesz J.J., Strehlow R.A**. Explosion Hazards and Evaluation. Elsevier, Amsterdam, 1983.
3. **UFC 3-340-02**. Structures to Resist the Effects of Accidental Explosions. U.S. Department of Defense, 2008.
4. **Smith P.D., Hetherington J.G.** Blast and Ballistic Loading of Structures. Butterworth-Heinemann, Oxford, 1994.
5. **Ngo T., Mendis P., Gupta A., Ramsay J**. Blast loading and blast effects on structures – an overview. Electronic Journal of Structural Engineering, 2007, 7, pp. 76–91.
6. **European Commission, Joint Research Centre.** Survey on blast effects and fragment-induced injuries. Luxembourg: Publications Office of the European Union, 2018, pp. 5–6.
7. **Committee for the Prevention of Disasters.** Methods for the determination of possible damage to people and objects resulting from the releases of hazardous materials (TNO Green Book). The Hague: Directorate-General of Labour, 1982.
8. **Courtney A., Courtney M.** Links between traumatic brain injury and ballistic pressure waves. Brain Injury, 2009, 23 (6), pp. 657–662.
9. **Bass C.R., Panzer M.B., Rafaels K.A., Wood G., Shridharani J., Capehart B**. Brain injuries from blast. Journal of Biomechanics, 2012, 45 (1), pp. 1–12.
10. **Rafaels K.A., Bass C.R., Panzer M.B**. Brain injury risk from primary blast. Journal of Trauma, 2010, 69 (2), pp. 413–420.
11. **Panzer M.B., Myers B.S., Capehart B.P., Bass C.R.** Development of a finite element model for blast brain injury. Annals of Biomedical Engineering, 2012, 40 (7), pp. 1530–1544.
12. **Dvořák P., Hejmal Z., Dubec B., Holub J.** Use of pencil probes for blast pressure measurement. In: Proceedings of the International Conference on Military Technologies (ICMT 2021). Brno: University of Defence, 2021, pp. 1–4.
13. **Štoller J., Zezulová E.** Testing of critical infrastructure protection against the distant trinitrotoluene blast. In: Transport Means 2015, Proceedings of the 19th International Scientific Conference. Kaunas: Kaunas University of Technology, 2015, pp. 505–508.
14. **Zezulová E., Štoller J.** The field testing of high performance fiber reinforced concrete slabs under the TNT load explosion together with the analytical solution and the numerical modelling of those tests results. In: Proceedings of the International Conference on Military Technologies (ICMT 2015). Brno: University of Defence, 2015, pp. 211–218.
15. **Codina R., Ambrosini D.** Full-scale testing of leakage of blast waves inside a partially vented room exposed to external air blast loading. Shock Waves, 2018, 28, pp. 227–241.
16. **Gajewski T., Sielicki P.W.** Experimental study of blast loading behind a building corner. Shock Waves, 2020, 30, pp. 385–394.
17. **Rigby S.E., Tyas A., Bennett T**. Reflection and clearing of blast waves in confined spaces. Shock Waves, 2014, 24, pp. 495–506.
18. **Shin J., Krauthammer T.** Behavior of structural members subjected to internal blast loading. Engineering Structures, 2006, 28, pp. 154–165.
19. **Luccioni B.M., Ambrosini R.D., Danesi R.F**. Analysis of building collapse under blast loads. Engineering Structures, 2004, 26, pp. 63–71.
20. **Held M.** Blast Waves and Their Effects. Springer, Berlin, 1985.